Published in final edited form as:
Hum Mutat. 2010 February ; 31(2): 167–175. doi:10.1002/humu.21166.

XPC branch-point sequence mutations disrupt U2 snRNP binding resulting in abnormal pre-mRNA splicing in xeroderma pigmentosum patients

Sikandar G. Khan[1], **Koji Yamanegi**[2,3], **Zhi-Ming Zheng**[2], **Jennifer Boyle**[1,4], **Kyoko Imoto**[1,5], **Kyu-Seon Oh**[1], **Carl C. Baker**[6], **Engin Gozukara**[7,8], **Ahmet Metin**[9,10], and **Kenneth H. Kraemer**[1]

[1]Dermatology Branch, Center for Cancer Research, National Cancer Institute, Bethesda, MD

[2]HIV and AIDS Malignancy Branch, Center for Cancer Research, National Cancer Institute, Bethesda, MD

[6]Laboratory of Cellular Oncology, Center for Cancer Research, National Cancer Institute, Bethesda, MD

[7]Department of Biochemistry, Inonu University Medical School, Malatya, Turkey

[9]Department of Dermatology, Yuzuncu Yil University Medical School, Van, Turkey

Abstract

Mutations in two branch-point sequences (BPS) in intron 3 of the *XPC* DNA repair gene affect pre-mRNA splicing in association with xeroderma pigmentosum (XP) with many skin cancers (XP101TMA) or no skin cancer (XP72TMA), respectively. To investigate the mechanism of these abnormalities we now report that transfection of minigenes with these mutations revealed abnormal *XPC* pre-mRNA splicing that mimicked pre-mRNA splicing in the patients' cells. DNA oligonucleotide-directed RNase H digestion demonstrated that mutations in these BPS disrupt U2 snRNP – BPS interaction. XP101TMA cells had no detectable XPC protein but XP72TMA had 29% of normal levels. A small amount of XPC protein was detected at sites of localized UV-damaged DNA in XP72TMA cells which then recruited other nucleotide excision repair (NER) proteins. In contrast, XP101TMA cells had no detectable recruitment of XPC or other NER proteins. Post-UV survival and photoproduct assays revealed greater reduction in DNA repair in XP101TMA cells than in XP72TMA. Thus mutations in *XPC* BPS resulted in disruption of U2 snRNP-BPS interaction leading to abnormal pre-mRNA splicing and reduced XPC protein. At the cellular level these changes were associated with features of reduced DNA repair including diminished NER protein recruitment, reduced post-UV survival and impaired photoproduct removal.

Keywords

XPC; DNA repair; pre-mRNA splicing; xeroderma pigmentosum; skin cancer; U2 snRNP

Corresponding Author: Kenneth H. Kraemer, M.D. Chief, DNA Repair Section, Dermatology Branch Center for Cancer Research, National Cancer Institute Building 37 Room 4002, Bethesda, MD 20892 -4258 301-496-9033 FAX: 301-594-3409 kraemerk@nih.gov.
[3]Current affiliation: Department of Pathology, Hyogo College of Medicine, Hyogo, Japan
[4]Current affiliation: National Institute for Biological Standards and Control, Hertfordshire, United Kingdom
[5]Current affiliation: Department of Dermatology, Nara Medical University, Nara, Japan
[8]Curent affiliation: Dr. Fethiye Ersan Test-Tube Baby and Genetic Diagnosis Center, Malatya, Turkey
[10]Current affiliation: Department of Dermatology, Ankara Ataturk Research and Training Hospital, Ankara, Turkey

INTRODUCTION

The expression of eukaryotic genes requires the removal of introns and joining of the flanking exons by pre-mRNA splicing [Maniatis and Reed, 1987; Wu and Manley, 1989; Lopez, 1998; Hastings and Krainer, 2001; Faustino and Cooper, 2003; Zheng, 2004; Patel and Bellini, 2008; Niu, 2008]. RNA splicing is carried out by assembly of spliceosomes on the pre-mRNA. The branch point sequence (BPS), the polypyrimidine tract (Py tract), and the conserved dinucleotide AG at the 3' splice site are critical for the pre-mRNA splicing. In recent years mutations at these sites have been reported that influence the splicing of pre-mRNA [Lopez, 1998; Vervoort et al., 1998; Khan et al., 2004; Sinnreich et al., 2006; Zhang et al., 2008] and references therein]. However, the association of BPS mutations with the mechanism of clinical disease has not been clearly understood.

Xeroderma pigmentosum (XP) is a rare autosomal recessive disorder with a 1000-fold increase in skin cancer frequency in association with defective DNA repair [Kraemer et al., 1994; Kraemer et al., 2007; Kraemer and Ruenger, 2008; Ruenger et al., 2008]. Cells from XP patients are hypersensitive to killing by UV radiation and have defects in the nucleotide excision repair (NER) pathway that serves to remove UV induced DNA damage (cyclobutane pyrimidine dimers (CPD) and 6-4 photoproducts (6-4 PP)) [Friedberg et al., 2006; Khan et al., 2009]. XP cells fall into seven genetic complementation groups XP-A through XP-G. XP-C is one of the more common forms in the United States. The *XPC* DNA repair gene [MIM# 278720] encodes a 940 amino acid protein [NP_004619] that forms an in vivo stable heterotrimeric complex with one of the two human orthologs of *Saccharomyces cerevisiae* Rad23p (hHR23A or hHR23B) and centrin 2, a component of the centrosome. XPC functions as a DNA-damage sensor and repair recruitment factor in global genome repair by monitoring the DNA double helix for non-hydorgen bonded bases and then trapping undamaged nucleotides without direct contact with the DNA photoproduct. [Camenisch et al., 2009]. Most patients with defects in the *XPC* gene have undectable levels of XPC protein [Chavanne et al., 2000; Khan et al., 2006; Khan et al., 2009].

Our previous studies demonstrated that cells from two severely affected XP siblings had undetectable levels of *XPC* mRNA, while the cells from three mildly affected siblings had 3-5 % of normal levels [Khan et al., 2004]. These cells have mutations within two different BPS in the *XPC* intron 3 [Khan et al., 2004]. This intron thus has two functional BPS, possibly in order to compensate for a very weak splice acceptor [Khan et al., 2002]. Understanding of the interaction of constitutive splice site elements with factors such as U1 and U2 snRNPs, SF1 and U2AF can be enhanced by studies involving alternative splicing [Maniatis and Reed, 1987; Wu and Manley, 1989; Faustino and Cooper, 2003; Kyburz et al., 2006; Patel and Bellini, 2008; Niu, 2008]. We here extend our earlier studies to show that the two BPS in intron 3 of the *XPC* gene are functional for the efficient and accurate splicing of *XPC* pre – mRNA. We also found that the different levels of functional XPC protein correlated with different levels of DNA repair in the cells and with the severity of skin cancer involvement in these XP patients.

MATERIALS AND METHODS

Cell lines, culture conditions and DNA/RNA isolation

Fibroblast and lymphoblastoid cell cultures from Turkish family A: XP101TMA (GM15715, GM15716) and XPH102TMA (GM15717, GM15718); family B: XP72TMA (GM14877, GM14876A); normal fibroblasts (AG13145, AG04659, AG13354 and AG13129) and lymphoblastoid (KR06057) cells were obtained from the Human Genetic Mutant Cell Repository (Camden, NJ). SV40-transformed XP-C fibroblast (XP4PA-SV) cells were a gift from Dr. R. Legerski (M. D. Anderson Hospital, Houston, TX). These cell lines were

cultured and the separation of RNA and DNA was performed as described [Khan et al., 2006].

Construction of minigenes

To construct different expression vectors containing either wild-type BPS or mutated BPS, genomic DNA from normal or patients cells harboring these regions were amplified using an overlapping PCR technique [Zheng et al., 2000; Yamanegi et al., 2005] (see Figure 1 and Supp. Methods).

In vivo XPC pre-mRNA splicing assay

The plasmids either with normal BPS or mutated BPS were transfected into 0.3×10^6 XP4PA-SV fibroblasts using lipofectamine (Invitrogen) [Li et al., 1993; Khan et al., 2002]. Total cellular RNA was extracted after 48 hr employing RNAqueous small scale phenol-free total RNA isolation kit (Ambion). Following RNase-free DNase I digestion, 1 μg of total RNA was reverse-transcribed and different XPC mRNA isoforms were measured by real-time QRT-PCR using isoform-specific primer pairs (Table 1)[Khan et al., 2002]. We used CMV upstream primer (5'-CACTGCTTACTGGCTTATCG-3') [Fujimori et al., 2001] located in pcDNA3.1/V5 vector and *XPC* gene specific reverse primers, oVMM-22 (for exon 4 inclusion) and oCCB-364 (for exon 4 skipping). The use of the CMV upstream forward primer amplified the template expressed solely from minigenes. This primer sequence is present only in the *XPC* messages expressed from the minigenes but not from endogenously expressed *XPC* mRNA in the cells. Real time QRT-PCR assays were carried out on a Bio-Rad iCycler iQ system (Bio-Rad, Hercules, CA, USA) using 2x Bio-Rad IQ SYBR Green supermix (Bio-Rad, Hercules, CA, USA).

In vitro RNA transcription, RNase H cleavage protection assay and U2 snRNP depletion

To prepare DNA templates for *in vitro* transcription, genomic DNA from patients and normal cells were used to amplify the target regions employing an overlapping PCR technique and the PCR fragments were sub-cloned into pcDNA3.1/V5 expression vector. The *in vitro* transcription of the purified DNA templates employing gene specific primer oKY40 (5'-CAATCTCTATCTCCACT GGCTTC-3', 10349-10327) and T7 RNA polymerase was performed in the presence of [alpha-^{32}P] GTP to label the entire probe using the Riboprobe system (Promega, Madison, WI)[Yamanegi et al., 2005]. Individual single-strand DNA oligonucleotides complementary to either normal BPS or mutant BPS were used for oligonucleotide-directed Rnase H digestion assay (Figure 2A and B) [Yamanegi et al., 2005]. The following antisense DNA oligonucleotides were used: oKY41 (5'-ATCAACAAGCATT-3', 10257-10245), complementary to intron 3 with a wild type -4 BPS XPC pre-mRNA; oKY42 (5'-ATCAACTA GCATT-3', 10257-10245), complementary to intron 3 with a -9 T to A mutation within -4 BPS); oKY43 (5'-AATCAGTAATAGT-3', 10238-10226) complementary to intron 3 with a wild type -24 BPS XPC pre-mRNA; oKY44 (5'-AACCAGTAATAGT-3', 10238-10226), complementary to intron 3 with a mutant -24 BPS XPC pre-mRNA.

In order to confirm the specificity of the U2 snRNP-BPS interactions, the U2 snRNP from the HeLa nuclear extract was first depleted using U2 (oKY7, 5'-AGGCCGAGAAGCGA-3') oligonucleotide-mediated RNase H digestion [Yamanegi et al., 2005] and then used in the reaction mixture for the RNase H cleavage protection assay (Figure 2A).

Detection of XPC protein

Western blotting of the XPC as well as β-Actin proteins were performed by use of XPC specific monoclonal (ab6264) (Abcam, Inc., Cambridge, MA) and anti-β-Actin polyclonal (Santa Cruz) antibodies [Khan et al., 2006].

Local UV irradiation, immunofluorescence and confocal microscopy

The primary fibroblasts from normal and XP-C patients were cultured for 3 days to allow efficient uptake of the different size of beads (0.8 μm and 2.0 μm respectively, carboxylate microspheres, Polysciences Inc.). The cells with different sized beads were grown (in a 1:1 ratio) on the coverslips for 24 hr in a 35 mm dish and were overlaid with 5 μm Millipore filters for localized irradiation with 100 J/m^2 UVC. The localization of core NER proteins in the cells at the site of DNA lesions was detected using immunocytochemistry and confocal laser-scanning [Jaspers and Bootsma, 1982; Volker et al., 2001; Oh et al., 2007; Boyle et al., 2008; Khan et al., 2009]. Fifty nuclei were evaluated per sample [Boyle et al., 2008].

Measurement of UV sensitivity

UV sensitivity was determined using a 3-(4, 5-dimethylthiazol-2-yl)-5-(3-carboxymethoxyphenyl)-2-(4-sulfophenyl)-2 H-tetrazolium (MTS) assay (Promega)[Imoto et al., 2002].

Measurement of UV-induced photoproducts

Cells were UV-irradiated and 6-4 PP and CPD were quantified by an enzyme-linked immunosorbent assay (ELISA) using 64M-2 and TDM-2 monoclonal antibodies [Nakagawa et al., 1998; Imoto et al., 2002; Nishiwaki et al., 2004].

RESULTS

In vivo RNA splicing using minigenes containing mutations within BPS mimics the abnormal splicing in the XP-C patients' cells

The XP101TMA cells had a -9 T to A change within the -4 BPS [c.413-9T>A; g.10251T>A; Accessions: NM_004628.3; NC_000003.10] and the XP72TMA cells had a -24 A to G change within the -24 BPS [c.413-24A>G; g.10236A>G] both in the *XPC* intron 3 [Khan et al., 2004]. To confirm that these mutations produced abnormal splicing, we transfected minigenes containing three exons (exons 3, 4 and 5.1) with either normal or mutated BPS sequences into XP4PA-SV fibroblasts (Figure 1A). We used a sensitive real-time quantitative RT-PCR assay to measure the expression of both exon 4 inclusion as well as exon 4 skipped messages [Khan et al., 2002]. The *in vivo* pre-mRNA splicing assay using normal and mutant minigene constructs showed that the mutations within -4 BPS or -24 BPS in the *XPC* intron3 resulted in abnormal *XPC* pre-mRNA splicing (Table 1). The use of CMV upstream primer permitted measurement only of the expressed messages from the minigenes. The location of the pair primers used to measure the inclusion of exon 4 and skipping of exon 4 exclusively expressed by minigene transfection in the XP-C cells are digramatically shown in Figure 1B. Transfection of XP4PA-SV cells with the minigene containing normal sequences resulted in 27,550 fg exon 4 inclusion message (Table 1). The minigene harboring the -24 change (A to G) lowered the expression of exon 4 inclusion message (5,185 fg -19 %) compared to the minigene with the normal sequence. There was a greater reduction in the expression of the exon 4 inclusion message (1,380 fg – 5 %) with the minigene harboring the -9 mutation (T to A). These minigene results are consistent with the results in the cells from the mild (XP72TMA) and severe (XP101TMA) patients (Table 1). These results indicate that both BPS function in *XPC* pre-mRNA splicing. This clearly reveals the effects of these branch point mutations on normal splicing of XPC message.

These results further indicate that these minigene constructs mimic some of the behavior of the endogenous *XPC* pre-mRNA.

However, the ratio of exon 4 inclusion / skipping in the *XPC* message using normal – BPS minigene (4.6) was less than with the normal cells (39.8) (Table 1 last column) suggesting that these constructs lack some unknown regulatory elements and/or have shorter sized introns that may be critical for accurate and efficient splicing of *XPC* pre – mRNA [Berget, 1995;Reed, 1996;Dewey et al., 2006]. Thus these minigenes do not fully duplicate the splicing of the endogenous *XPC* pre-mRNA.

Quantitative analysis of U2 snRNP-BPS interactions in XPC pre-mRNA by use of DNA oligo-directed RNase H digestion

We used an RNase H protection assay to assess the effect of mutations on the binding of U2 snRNP to XPC pre-mRNA (Figures 1C and 2A). ^{32}P-labeled two exon (exons 3 and 4) minigene pre-mRNA (containing either wild type, -24 A to G, or -9 T to A mutations) (Figure 2B) was incubated with a nuclear extract either containing U2 snRNP or with U2 snRNP depleted. A single stranded DNA oligonucleotide complementary to the target sequence was added. Binding of U2 snRNP with BPS will prevent the binding of the oligonucleotide to the target BPS. RNase H will digest RNA in RNA:DNA duplex and single stranded RNA that is adjacent to the duplex [Lima and Crooke, 1997] and thus indicates the extent of binding by U2 snRNP (Figure 2A).

The DNA oligonucleotide-directed RNase H digestion assay indicates that the *XPC* pre-mRNA intron 3 with wild-type -24BPS (Figure 2C lanes 7, 8, 17, and 18) had stronger binding (0 % digestion) for U2 snRNP than did the *XPC* pre-mRNA intron 3 with mutated -24BPS (Figure 2C lanes 9, 10, 19, and 20) (27% to 40% digestion) whether the oligo was added simultaneously or 10 min after the nuclear extract or whether incubated for 10 min or 30 min. The *XPC* pre-mRNA intron 3 with wild-type -9 sequence (Figure 2C lanes 2, 3, 12, and 13) showed more RNase H digestion (36% to 72% digestion) than the wild type -24 sequence indicating weaker binding for U2 snRNP. Specific binding of U2 snRNP appeared at both BPS since depletion of U2 snRNP increased the extent of RNase H digestion for both BPS (Figure 2C compare lane 7 – 0% to lane 24 – 18% and lane 2 – 57% to lane 22 – 85%). The wild-type genomic DNA sequences of the XPC intron 3 / exon 4 junction with two functional BPSs located at -4 and -24 positions are shown in Figure 1D. Since the binding of U2 snRNP with the -24 BPS was more pronounced than with the -4BPS, the -24 BPS may be the predominant BPS in *XPC* pre-mRNA splicing.

The *XPC* pre-mRNA intron 3 with the -9 T to A mutation showed less RNase H digestion (Figure 2C lanes 4, 5, 14, and 15) (24% to 39% digestion) than the wild type – 9 sequence (Figure 2C lanes 2, 3, 12, and 13) (36% to 72% digestion), suggesting that the -9 T to A mutation might create a binding site for other unknown factors. Depletion of U2 snRNP increased RNase H digestion of the -9 T to A change only by a small amount (Figure 2C compare lane 5 – 39% to lane 23 – 44%), further suggesting that another binding factor may be present in the nuclear extract that binds to the -9 mutated sequence.

Association of XPC protein levels in the patients' cells with their clinical phenotypes

Most XP-C patients with multiple sunlight induced skin cancers have undectable levels of XPC protein while their cancer-free parents (who are obligate heterozygotes) have normal levels [Chavanne et al., 2000; Khan et al., 2006; Khan et al., 2009]. The level of XPC protein in the severely-affected patient, XP101TMA, was not detectable, while in cells from mildly-affected patient, XP72TMA, reduced expression (~29 %) of normally migrating XPC protein was present (Figure 3C). Cells from the clinically normal parent of the severely

affected patient (XP-C heterozygote, XPH102TMA) showed a strong band indicating normal expression of XPC protein.

In vivo interactions between NER components in the patients' cells

XPC is a DNA damage sensor and recruitment factor for other NER proteins in global genome repair [Camenisch et al., 2009]. Mixed cultures of normal cells (labeled with 0.8 μm beads) and patient cells (labeled with 2.0 μm beads) were UV-irradiated through 5μm diameter pores of a polycarbonate isopore membrane filter to directly examine the localization of repair proteins involved in NER to sites of DNA damage *in vivo*. The NER components were detected by immunofluorescence and confocal laser-scanning microscopy [Volker et al., 2001; Oh et al., 2007; Boyle et al., 2008; Khan et al., 2009]. In the absence of UV treatment XPC and XPG protein was detectable in the normals cells (Figure 3A and 3B top row, red arrows). Long exposure of the confocal image revealed the presence of XPC protein in the XP72TMA cells (Figure 3A – top row, yellow arrow) but not in the XP101TMA cells (Figure 3B – top row), consistent with the results of the Western blots (Figure 3C). XPG protein was visualized in the XP72TMA (Figure 3A – top row, yellow arrow) and XP101TMA (Figure 3B – top row, yellow arrow) cells at short exposure of the confocal image, demonstrating presence of this NER protein in these cells.

Following exposure to localized UV, DNA damage was visualized by the presence of fluorescent foci of CPD (Figure 3A bottom row, right image, red and yellow arrows) and 6-4 PP (Figure 3A third row, right image, red and yellow arrows) in the normal and XP72TMA cells. XPC protein was visualized at the site of the DNA damage in the normal cells (Figure 3A, second row, left image, red arrow). In the XP72TMA cells long exposure of the confocal image revealed localized XPC protein (Figure 3A, second row, middle image, yellow arrow) reflecting a low level of functioning XPC protein. Recruitment of XPG, XPA, XPB, XPD and XPF proteins to the site of damage in the normal and XP72TMA cells was visualized at short exposure of the confocal image indicating functioning of this process (Figure 3A rows 2, 3, 4 and 5 red and yellow arrows) in the presence of low levels of XPC protein.

In contrast, XPC protein was not visualized in the XP101TMA cells before or after UV at short exposure of the confocal images (Figure 3B rows 1 and 2 left images) or at long exposure of the confocal image (not shown) under conditions where XPC protein was visualized in the normal cells (Figure 3B rows 1 and 2, left images, red arrows) and DAPI staining marked the cell nuclei in blue color (data not shown). XPG protein was visualized in the XP101TMA (Figure 3B row 1 right image, yellow arrow) and normal (Figure 3B, row 1 right image, red arrow) cells before UV. In contrast to the localization in the normal cell (Figure 3B, row 2, right image, red arrow) XPG protein did not localize to the site of DNA damage in the XP101TMA cells (Figure 3B, row 2, right image, yellow arrow). In the absence of binding of XPC protein to the DNA damaged site, the other NER components such as XPG (Figure 3B, row 2, right image, and data not shown) did not localize to the damaged site. This emphasizes the important role of XPC protein in recruiting other NER proteins to the site of DNA damage and indicates that a reduced level of XPC protein is sufficient to induce localization of the other NER proteins [Volker et al., 2001; Oh et al., 2007; Khan et al., 2009].

Reduced post-UV cell survival in the cell lines from mild and severe XP-C patients

To clarify the defective DNA repair in the patients' cells, we examined the UV sensitivities of normal as well as patients' cells using an MTS assay (Figure 4A). There was markedly reduced post-UV survival in cells from XP101TMA with severe disease (Figure 4A). Post-UV survival of XP72TMA cells from the patient with mild disease was greater than that in

the XP101TMA cells. The cell line from clinically normal mother of XP101TMA (XPH102TMA), an obligate XP heterozygote, showed UV sensitivities close to normal cells. These results indicate a relationship between DNA repair status of the cells and the clinical phenotypes in the XP patients.

Reduced repair of UV-induced photoproducts in genomic DNA from mild and severe patients' cells

To investigate whether the cells from the patients' that carry BPS mutations have defective global genome repair of the UV-induced DNA damage, we measured 6-4PP and CPD levels in genomic DNA at different time points after UV irradiation using an ELISA (Figure 4B and 4C). The normal fibroblasts had a rapid post-UV removal of 6-4 photoproducts (6-4 PP), with 5% remaining at 3 hr and 2% by 6 hr (Figure 4B) in keeping with earlier observations [Nishiwaki et al., 2004; Boyle et al., 2008; Khan et al., 2009]. The cells from the mildly-affected patient, (XP72TMA), showed nearly normal repair of 6-4 photoproducts in the genomic DNA compared to minimal 6-4 photoproduct repair in the cells from severely-affected patient, XP101TMA (Figure 4B). The XP72TMA cells had ~ 40% 6-4 PP by 3 hr and 18% at 6 hr, while XP101TMA had 94% 6-4 PP at 3 hr and ~ 89% by 6 hr. In normal cells the post-UV removal of cyclobutane pyrimidine dimer (CPD) photoproducts was slower with 56% remaining at 6 hr and 29% by 24 hr, which is consistent with previous reports [Boyle et al., 2008; Khan et al., 2009]. The removal of CPD in both patients' cells was delayed, again with greater delay in XP101TMA cells than in XP72TMA cells (Figure 4C). Thus, the cells from mildly-affected patient showed greater levels of repair of photoproducts than the severely-affected patient.

DISCUSSION

Disruption of the pre-mRNA splicing has been described for only a few diseases [Faustino and Cooper, 2003; Khan et al., 2004] and references therein. We previously reported that mutations in -4 and -24 branch-point sequences (BPS) in intron 3 of the XPC DNA repair gene differentially affect pre-mRNA splicing resulting in severe or mild disease [Khan et al., 2004]. The current paper investigates the mechanism of abnormal pre-mRNA splicing and the consequences in terms of reduction of XPC protein and DNA repair levels in these patients' cells.

The accurate and efficient splicing of the XPC pre-mRNA in the normal cells involving a very poor exon 4 splice acceptor (information content -0.1 bits) reveals the complexity of the XPC intron 3 sequences in pre-mRNA splicing [Khan et al., 2002]. In normal cells we were able to map two BPS at -4 and -24 positions in XPC intron 3 [Khan et al., 2004]. In contrast, cells from the mildly-affected patient showed only splice lariat intermediates with the -4BPS and the cells from the severely affected patient did not show splice lariat intermediates containing either BPS [Khan et al., 2004]. The detection of low levels of full-length XPC mRNA (Table 1) and XPC protein (Figure 3A and 3C) in cells from the mildly affected patient, XP72TMA, demonstrates utilization of the unmutated -4BPS in intron 3. The pre-mRNA splicing assay using normal and mutant minigene constructs also showed that the mutations within either of these two BPS in the *XPC* intron 3 resulted in abnormal XPC pre-mRNA splicing. Mutation at -24 BPS adenosine (-24A to G) resulted in the expression of more exon 4 inclusion message (19%) than mutation within -4 BPS (-9T to A change) (5%) (Table 1). This clearly demonstrates that the differential expression of the full-length *XPC* message in these patients' cells is associated with the mutation in two different BPS in intron 3 of the *XPC* gene. These results provide evidence that under some circumstances involvement of multiple BP sequences may be required for accurate and efficient splicing of human pre-mRNA.

The occurrence of abnormal *XPC* pre-mRNA splicing using minigenes with these BPS mutations further validated these *in vivo* patients' cellular findings. However, the enhanced skipping of exon 4 in the *XPC* message using minigenes with normal BPS, and expression of exon 4 inclusion message by use of minigene with -9 T to A change within -4 BPS (Table 1) indicates that these constructs lack some unknown cis-acting regulatory elements such as intronic activators or repressors that are required for the specificity in pre-mRNA splicing [Berget, 1995;Reed, 1996;Faustino and Cooper, 2003]. Alternatively the shorter size of the introns may influence the pre-mRNA splicing [Berget, 1995;Reed, 1996;Dewey et al., 2006].

The U2 snRNP binds the BPS via RNA : RNA interactions between the snRNA and the pre-mRNA, and this step is critical for pre-mRNA splicing [Wu and Manley, 1989; Wu and Manley, 1991; Berget, 1995; Reed, 1996; Faustino and Cooper, 2003; Kyburz et al., 2006; Patel and Bellini, 2008; Niu, 2008]. The analysis of the interaction of U2 snRNP with normal and mutant BPS of the *XPC* pre-mRNA intron 3 revealed that both the BPS in the *XPC* intron 3 are functional but -24 BPS predominates by interacting more strongly with U2 snRNP. The stronger binding of U2 snRNP with -24 BPS than -4 BPS is in agreement with higher BPS information content of -24 BPS (9.3 bits) than -4 BPS (0.4 bits) as described [Khan et al., 2004]. In spite of stronger binding of U2 snRNP with -24 BPS than -4 BPS, XP-C patients harboring mutation within -4 BPS are severely-affected and those with -24 BPS mutation are mildly-affected [Khan et al., 2004]. This may be explained by the fact that the mutation within the -4 BPS reduces the information content of the XPC exon 4 splice acceptor to -2.3 bits. This is a greater reduction than the -24 BPS mutation which reduces the exon 4 splice acceptor information content to -0.4 bits. Mutations within -4 BPS or -24 BPS may disrupt the U2 snRNP-BPS interaction either through interfering with the putative Py tract (a run of five uridines in *XPC* intron 3) function or via disrupting the interaction of some unknown splicing factor(s) near these BPS [Khan et al., 2002; Khan et al., 2004]. The minimal increase in the RNase H digestion with the -9 T to A mutation (Figure 2C) suggests that some unknown factor(s) may bind to this site affecting use of the exon 4 acceptor resulting in complete disruption of normal *XPC* pre-mRNA splicing in the cells from the severe patients. The milder patient utilizes the normal weak -4 BPS during the course of *XPC* pre-mRNA splicing resulting in the expression of minimal amounts of both full-length *XPC* mRNA and XPC protein.

The very low level of normal (exon 4 inclusion) XPC mRNA transcript (3%) (Table 1) resulted in 29% of normal level of normal sized XPC protein (Figure 3C) in the XP72TMA cells. This suggests that the moderate phenotype of XP72TMA is related to the presence of some normal XPC protein. Similarly, measurable amounts of normal transcripts of the *XPA* and *XPD* DNA repair genes in mildly-affected patients have been reported recently [Sidwell et al., 2006;Boyle et al., 2008;Botta et al., 2009].

In the cells from XP101TMA, we were unable to detect the localization of XPC protein at the site of the UV-induced DNA damage (Figure 3B). The failure to detect localization of XPC protein to UV damaged DNA is in agreement with the inability to detect XPC protein on western blotting (Figure 3C). In the absence of XPC protein, the other NER proteins did not localize to the damage site. This validates the other studies that revealed the interactions between the core components of NER at the site of damaged DNA, and supports the central role of XPC protein in DNA damage recognition and recruitment factors for the functional NER [Volker et al., 2001; Friedberg et al., 2006; Oh et al., 2007; Khan et al., 2009]. In contrast, long exposure of confocal image revealed the localization of a small amount of XPC protein at the sites of UV – induced DNA damage in the cells from XP72TMA (Figure 3A). This is in keeping with the small amount of *XPC* mRNA and protein in these cells.

However, there was recruitment of the other NER proteins in these cells indicating that these proteins require only a minimal amount of XPC binding to be recruited.

Post-UV survival of the cells from XP101TMA was much lower than that of XP72TMA (Figure 4A). ELISA assay of DNA photoproducts revealed virtually absent repair of 6-4 photoproducts (PP) in XP101TMA and nearly normal repair of 6-4 PP in XP72TMA (Figure 4B). Also the removal of CPD in case of XP72TMA was higher as compared to XP101TMA (Figure 4C). The absence of functional XPC protein in the patients' cells can increase the amount of un-repaired photoproducts in the DNA. The cells from mild and severe patients were differentially deficient in the repair of 6-4 as well as CPD photoproducts from genomic DNA, suggesting that these cells possess different degrees of DNA repair capabilities. Interestingly, the post-UV survival and DNA repair capabilities of these cells correlate well with XPC protein levels. This further suggests that UV-mediated effects can be modified to different degrees based on the amount of functional XPC proteins in the cells. We previously reported that the high frequency of skin cancer found in other XP-C patients [Khan et al., 2006], was associated with undetectable levels of XPC protein resulting from creation of premature termination codon (PTC) with consequent nonsense-mediated mRNA decay pathway [Khan et al., 2002; Maquat, 2005; Khan et al., 2006]. Taken together, these findings reinforce the significance of cellular DNA repair deficiency as a consequence of unavailability of XPC protein in causing multiple skin cancers in the XP-C patients. The presence of some normal XPC protein in the patient's cells might be rescuing otherwise more severe phenotypes resulting from the complete lack of functional XPC protein.

This study provides evidence that mutation in *XPC* BPS result in disruption of U2 snRNP-BPS interaction leading to abnormal XPC pre-mRNA splicing, reduced XPC protein, diminished NER protein recruitment, and reduced photoproduct removal in association with multiple skin cancers. The measurable amount of normal XPC message and functional XPC protein in some patients reflects the ability to repair some of the sun-induced DNA lesions providing a molecular basis for their milder clinical phenotype.

Acknowledgments

This research was supported by the Intramural Research Program of the NIH and the Center for Cancer Research of the National Cancer Institute. We thank Dr. Susan Garfield of CCR Confocal Microscopy Core Facility for assistance with the confocal microscopy and Ms. Najealicka Armstrong for assistance in the photoproduct assay.

REFERENCES

Berget SM. Exon recognition in vertebrate splicing. J Biol Chem. 1995; 270:2411–2414. [PubMed: 7852296]

Botta E, Nardo T, Orioli D, Guglielmino R, Ricotti R, Bondanza S, Benedicenti F, Zambruno G, Stefanini M. Genotype-phenotype relationships in trichothiodystrophy patients with novel splicing mutations in the XPD gene. Hum Mutat. 2009; 30:438–445. [PubMed: 19085937]

Boyle J, Ueda T, Oh KS, Imoto K, Tamura D, Jagdeo J, Khan SG, Nadem C, DiGiovanna JJ, Kraemer KH. Persistence of repair proteins at unrepaired DNA damage distinguishes diseases with ERCC2 (XPD) mutations: cancer-prone xeroderma pigmentosum vs. non-cancer-prone trichothiodystrophy. Hum Mutat. 2008; 29:1194–1208. [PubMed: 18470933]

Camenisch U, Trautlein D, Clement FC, Fei J, Leitenstorfer A, Ferrando-May E, Naegeli H. Two-stage dynamic DNA quality check by xeroderma pigmentosum group C protein. EMBO J. 2009; 28:2387–2399. [PubMed: 19609301]

Chavanne F, Broughton BC, Pietra D, Nardo T, Browitt A, Lehmann AR, Stefanini M. Mutations in the XPC gene in families with xeroderma pigmentosum and consequences at the cell, protein, and transcript levels. Cancer Res. 2000; 60:1974–1982. [PubMed: 10766188]

Dewey CN, Rogozin IB, Koonin EV. Compensatory relationship between splice sites and exonic splicing signals depending on the length of vertebrate introns. BMC Genomics. 2006; 7:311. [PubMed: 17156453]

Faustino NA, Cooper TA. Pre-mRNA splicing and human disease. Genes Dev. 2003; 17:419–437. [PubMed: 12600935]

Friedberg, EC.; Walker, GC.; Siede, W.; Wood, RD.; Schultz, RA.; Ellenberger, T. DNA Repair and Mutagenesis. ASM Press; Washington, D.C.: 2006.

Fujimori A, Tachiiri S, Sonoda E, Thompson LH, Dhar PK, Hiraoka M, Takeda S, Zhang Y, Reth M, Takata M. Rad52 partially substitutes for the Rad51 paralog XRCC3 in maintaining chromosomal integrity in vertebrate cells. EMBO J. 2001; 20:5513–5520. [PubMed: 11574483]

Hastings ML, Krainer AR. Pre-mRNA splicing in the new millennium. Curr Opin Cell Biol. 2001; 13:302–309. [PubMed: 11343900]

Imoto K, Kobayashi N, Katsumi S, Nishiwaki Y, Iwamoto TA, Yamamoto A, Yamashina Y, Shirai T, Miyagawa S, Dohi Y, Sugiura S, Mori T. The total amount of DNA damage determines ultraviolet-radiation-induced cytotoxicity after uniformor localized irradiation of human cells. J Invest Dermatol. 2002; 119:1177–1182. [PubMed: 12445209]

Jaspers NG, Bootsma D. Genetic heterogeneity in ataxia-telangiectasia studied by cell fusion. Proc Natl Acad Sci U S A. 1982; 79:2641–2644. [PubMed: 6953420]

Khan SG, Metin A, Gozukara E, Inui H, Shahlavi T, Muniz-Medina V, Baker CC, Ueda T, Aiken JR, Schneider TD, Kraemer KH. Two essential splice lariat branchpoint sequences in one intron in a xeroderma pigmentosum DNA repair gene: mutations result in reduced XPC mRNA levels that correlate with cancer risk. Hum Mol Genet. 2004; 13:343–352. [PubMed: 14662655]

Khan SG, Muniz-Medina V, Shahlavi T, Baker CC, Inui H, Ueda T, Emmert S, Schneider TD, Kraemer KH. The human XPC DNA repair gene: arrangement, splice site information content and influence of a single nucleotide polymorphism in a splice acceptor site on alternative splicing and function. Nucleic Acids Res. 2002; 30:3624–3631. [PubMed: 12177305]

Khan SG, Oh KS, Emmert S, Imoto K, Tamura D, DiGiovanna JJ, Shahlavi T, Armstrong N, Baker CC, Neuburg M, Zalewski C, Brewer C, Wiggs E, Schiffmann R, Kraemer KH. XPC initiation codon mutation in xeroderma pigmentosum patients with and without neurological symptoms. DNA Repair (Amst). 2009; 8:114–125. [PubMed: 18955168]

Khan SG, Oh KS, Shahlavi T, Ueda T, Busch DB, Inui H, Emmert S, Imoto K, Muniz-Medina V, Baker CC, DiGiovanna JJ, Schmidt D, Khadavi A, Metin A, Gozukara E, Slor H, Sarasin A, Kraemer KH. Reduced XPC DNA repair gene mRNA levels in clinically normal parents of xeroderma pigmentosum patients. Carcinogenesis. 2006; 27:84–94. [PubMed: 16081512]

Kraemer KH, Lee MM, Andrews AD, Lambert WC. The role of sunlight and DNA repair in melanoma and nonmelanoma skin cancer. The xeroderma pigmentosum paradigm. Arch Dermatol. 1994; 130:1018–1021. [PubMed: 8053698]

Kraemer KH, Patronas NJ, Schiffmann R, Brooks BP, Tamura D, DiGiovanna JJ. Xeroderma pigmentosum, trichothiodystrophy and Cockayne syndrome: A complex genotype-phenotype relationship. Neuroscience. 2007; 145:1388–1396. [PubMed: 17276014]

Kraemer, KH.; Ruenger, TM. Genome instability, DNA repair and cancer.. In: Wolff, K.; Goldsmith, LA.; Katz, SI.; Gilchrest, BA.; Paller, AS.; Leffell, DJ., editors. Fitzpatrick's Dermatology in General Medicine. McGraw Hill; New York: 2008. p. 977-986.

Kyburz A, Friedlein A, Langen H, Keller W. Direct interactions between subunits of CPSF and the U2 snRNP contribute to the coupling of pre-mRNA 3′ end processing and splicing. Mol Cell. 2006; 23:195–205. [PubMed: 16857586]

Li L, Bales ES, Peterson CA, Legerski RJ. Characterization of molecular defects in xeroderma pigmentosum group C. Nat Genet. 1993; 5:413–417. [PubMed: 8298653]

Lima WF, Crooke ST. Cleavage of single strand RNA adjacent to RNA-DNA duplex regions by Escherichia coli RNase H1. J Biol Chem. 1997; 272:27513–27516. [PubMed: 9346880]

Lopez AJ. Alternative splicing of pre-mRNA: Developmental consequences and mechanisms of regulation. Annu Rev Genet. 1998; 32:279–305. [PubMed: 9928482]

Maniatis T, Reed R. The role of small nuclear ribonucleoprotein particles in pre-mRNA splicing. Nature. 1987; 325:673–678. [PubMed: 2950324]

Maquat LE. Nonsense-mediated mRNA decay in mammals. J Cell Sci. 2005; 118:1773–1776. [PubMed: 15860725]

Nakagawa A, Kobayashi N, Muramatsu T, Yamashina Y, Shirai T, Hashimoto MW, Ikenaga M, Mori T. Three-dimensional visualization of ultraviolet-induced DNA damage and its repair in human cell nuclei. J Invest Dermatol. 1998; 110:143–148. [PubMed: 9457909]

Nishiwaki Y, Kobayashi N, Imoto K, Iwamoto TA, Yamamoto A, Katsumi S, Shirai T, Sugiura S, Nakamura Y, Sarasin A, Miyagawa S, Mori T. Trichothiodystrophy fibroblasts are deficient in the repair of ultraviolet-induced cyclobutane pyrimidine dimers and (6-4)photoproducts. J Invest Dermatol. 2004; 122:526–532. [PubMed: 15009740]

Niu DK. Exon definition as a potential negative force against intron losses in evolution. Biol Direct. 2008; 3:46. [PubMed: 19014515]

Oh KS, Imoto K, Boyle J, Khan SG, Kraemer KH. Influence of XPB helicase on recruitment and redistribution of nucleotide excision repair proteins at sites of UV-induced DNA damage. DNA Repair (Amst). 2007; 6:1359–1370. [PubMed: 17509950]

Patel SB, Bellini M. The assembly of a spliceosomal small nuclear ribonucleoprotein particle. Nucleic Acids Res. 2008; 36:6482–6493. [PubMed: 18854356]

Reed R. Initial splice-site recognition and pairing during pre-mRNA splicing. Curr Opin Genet Dev. 1996; 6:215–220. [PubMed: 8722179]

Ruenger, TM.; DiGiovanna, JJ.; Kraemer, KH. Hereditary Diseases of genome instability and DNA repair.. In: Wolff, K.; Goldsmith, LA.; Katz, SI.; Gilchrest, BA.; Paller, AS.; Leffell, DJ., editors. Fitzpatrick's Dermatology in General Medicine. McGraw Hill; New York: 2008. p. 1311-1325.

Sidwell RU, Sandison A, Wing J, Fawcett HD, Seet JE, Fisher C, Nardo T, Stefanini M, Lehmann AR, Cream JJ. A novel mutation in the XPA gene associated with unusually mild clinical features in a patient who developed a spindle cell melanoma. Br J Dermatol. 2006; 155:81–88. [PubMed: 16792756]

Sinnreich M, Therrien C, Karpati G. Lariat branch point mutation in the dysferlin gene with mild limb-girdle muscular dystrophy. Neurology. 2006; 66:1114–1116. [PubMed: 16606933]

Vervoort R, Gitzelmann R, Lissens W, Liebaers I. A mutation (IVS8+0.6kbdelTC) creating a new donor splice site activates a cryptic exon in an Alu-element in intron 8 of the human beta-glucuronidase gene. Hum Genet. 1998; 103:686–693. [PubMed: 9921904]

Volker M, Mone MJ, Karmakar P, van Hoffen A, Schul W, Vermeulen W, Hoeijmakers JH, van Driel R, van Zeeland AA, Mullenders LH. Sequential assembly of the nucleotide excision repair factors in vivo. Mol Cell. 2001; 8:213–224. [PubMed: 11511374]

Wu J, Manley JL. Mammalian pre-mRNA branch site selection by U2 snRNP involves base pairing. Genes Dev. 1989; 3:1553–1561. [PubMed: 2558966]

Wu JA, Manley JL. Base pairing between U2 and U6 snRNAs is necessary for splicing of a mammalian pre-mRNA. Nature. 1991; 352:818–821. [PubMed: 1831878]

Yamanegi K, Tang S, Zheng ZM. Kaposi's sarcoma-associated herpesvirus K8beta is derived from a spliced intermediate of K8 pre-mRNA and antagonizes K8alpha (K-bZIP) to induce p21 and p53 and blocks K8alpha-CDK2 interaction. J Virol. 2005; 79:14207–14221. [PubMed: 16254356]

Zhang K, Nowak I, Rushlow D, Gallie BL, Lohmann DR. Patterns of missplicing caused by RB1 gene mutations in patients with retinoblastoma and association with phenotypic expression. Hum Mutat. 2008; 29:475–484. [PubMed: 18181215]

Zheng ZM. Regulation of alternative RNA splicing by exon definition and exon sequences in viral and mammalian gene expression. J Biomed Sci. 2004; 11:278–294. [PubMed: 15067211]

Zheng ZM, Reid ES, Baker CC. Utilization of the bovine papillomavirus type 1 late-stage-specific nucleotide 3605 3′ splice site is modulated by a novel exonic bipartite regulator but not by an intronic purine-rich element. J Virol. 2000; 74:10612–10622. [PubMed: 11044105]

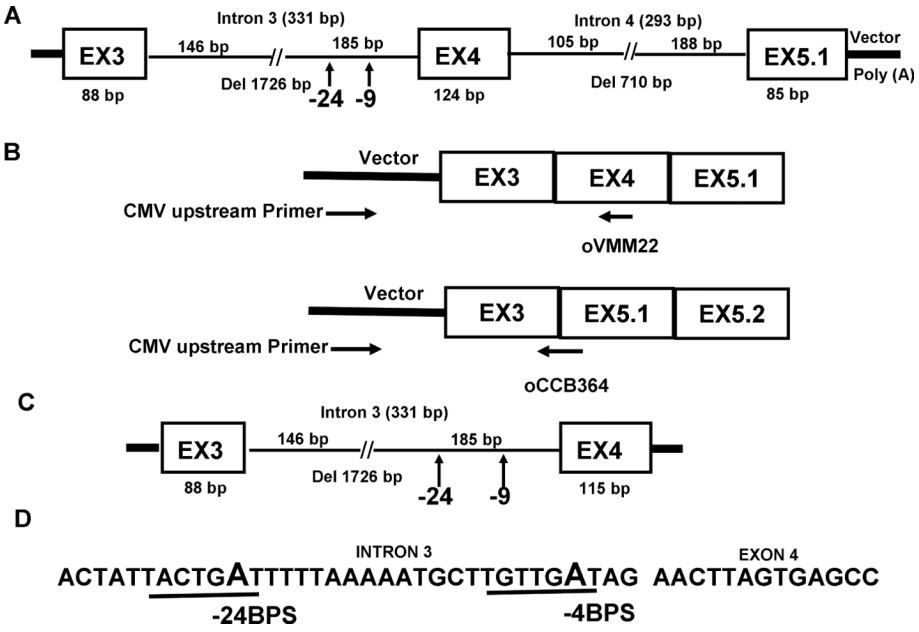

Figure 1.

XPC minigenes for pre-mRNA splicing and U2 snRNP/BPS binding; location of primers used for real-time QRT-PCR and the sequence of a portion of the genomic DNA of XPC intron 3 / exon 4 junction showing BPS. **A.** For the *in vivo* XPC pre-mRNA splicing studies minigenes containing three exons (3, 4 and 5.1) and partial intron3 and partial intron4 were constructed as described in materials and methods. B. Location of the primer used for real-time QRT-PCR to measure the exon 4 inclusion (Top panel) and exon 4 skipping (bottom panel). **C.** For U2 snRNP-BPS binding studies minigenes containing two exons (3 and 4) and partial intron3 were constructed as described in materials and methods. D. The sequence of a portion of the genomic DNA of the XPC intron 3/exon 4 junction is shown. The two BPS at -4 and -24 positions in the XPC intron are underlined and the BPS adenosine is denoted with a larger sized letter “A”.

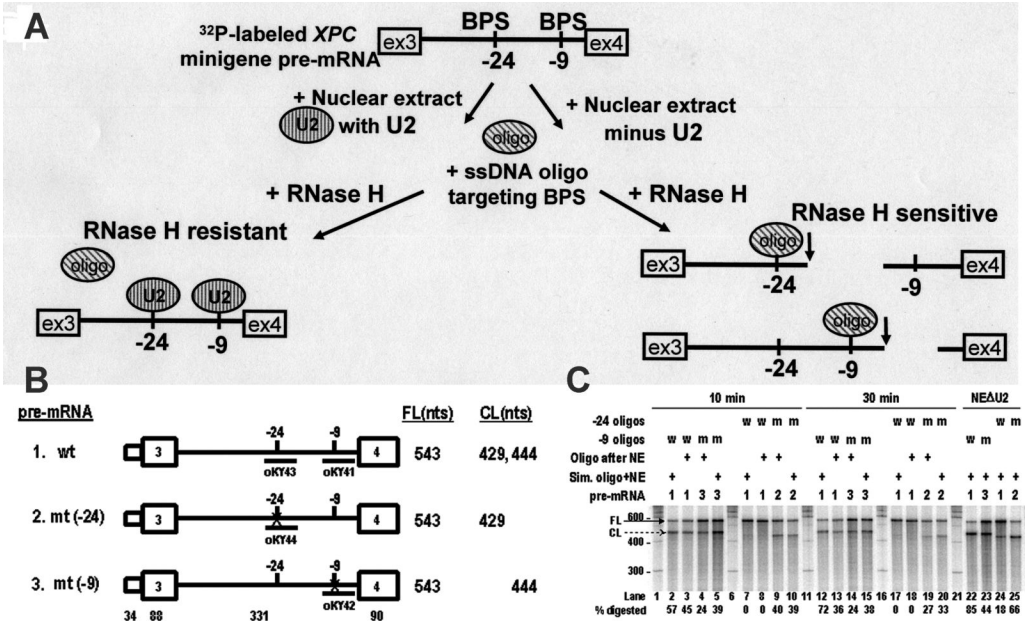

Figure 2.

Effect of mutations on U2 snRNP-BPS binding. A. Design of the U2 snRNP-BPS binding experiment. The ^{32}P-labeled *XPC* pre-mRNA was incubated for 10 min at 30°C with nuclear extract containing U2 snRNP or nuclear extract with U2 snRNP-depleted by using an U2 DNA oligo-mediated RNase H digestion. As RNase H cuts RNA in RNA:DNA duplex and single stranded RNA adjacent to RNA:DNA hybrids [Lima and Crooke, 1997], a strong U2 snRNP-BPS interaction (A) [Wu and Manley, 1989; Wu and Manley, 1991] prevents the BPS from base-pairing with the DNA oligonucleotide and thus resists RNase H digestion. U2 snRNP depletion experiments define the specificity of the BPS-U2 snRNP interactions. B. Diagram of the two exon XPC minigene pre-mRNAs and their cleavage products in DNA oligo-mediated RNase H digestion. The pre-mRNAs with 1. wt pre-mRNA, 2. mt -24 BPS (pre-mRNA), or 3. mt -9 within -4 BPS (pre-mRNA) was prepared by in vitro run-off transcription from the corresponding minigene plasmid in the presence of [alpha-^{32}P] GTP. X indicates the mutation. Showing on the right for each pre-mRNA are the size of the full-length (FL) pre-mRNA and its large cleavage (CL) product in a specific DNA oligo-mediated RNase H digestion. C. Quantitative analysis of U2 snRNP-BPS interactions of the *XPC* pre-mRNA intron 3 by DNA oligonucleotide-directed RNase H digestion. Gel image of RNase H digestion. The ^{32}P-labeled *XPC* pre-mRNA and nuclear extract were first incubated for 10 min or 30 min at 30° C in the absence of a single-stranded DNA oligonucleotide targeting to either wild-type or mutated BPS and then incubated for another 10 min in the presence of an oligonucleotide before digestion for 10 min with RNase H as described in Methods. The other set of reaction mixtures was incubated at 30° C for 10 min simultaneously in the presence of a specific DNA oligonucleotide and nuclear extract (with U2 snRNP or with U2 snRNP depleted) before digestion for 10 min with RNase H. The samples were resolved on 8% polyacrylamide gel containing 8M urea and a 100 bp DNA ladder as size marker in nts are shown in lanes 1, 6, 11, 16, and 21. The solid arrow indicates the undigested pre-mRNA and the dashed arrow indicates the large cleavage product. W, wt oligo for pre-mRNA 1; m, mt oligo for premRNA with a mt -24 BPS or a mt -4 BPS at -9 position; Sim. NE + oligo – simultaneous addition of nuclear extract and DNA oligonucleotide.

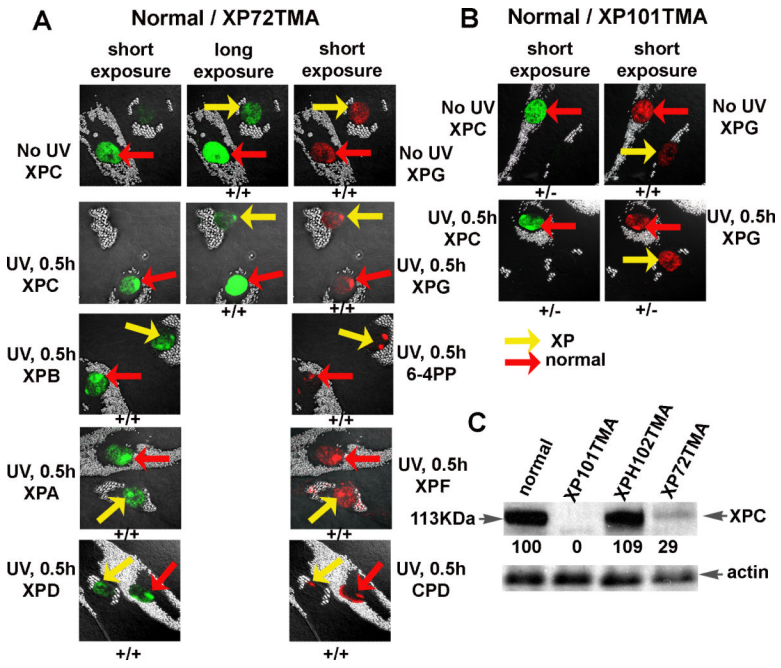

Figure 3.

Recruitment of XPC and other NER proteins to localized DNA damage in XP72TMA and XP101TMA cells following UV irradiation. The cytoplasm of normal cells (AG13145) was labeled with 0.8 μm latex beads and XP72TMA and XP101TMA cells were labeled with 2 μm latex beads. **A**. Normal and XP72TMA cells. Row 1. In the absence of UV, XPC and XPG proteins were stained in the normal and XP72TMA cells. Rows 2 – 5 – Following 100 J/m^2 UV irradiation delivered through a 5 μm filter, cells were fixed at 0.5h post-irradiation and immunostained with pairs of antibodies to simultaneously assess the location of DNA damage and NER proteins. The arrows indicate sites of localized immunostaining: normal red arrows, XP patients – yellow arrows. CPD photoproducts as well as the NER proteins (XPC, XPG, XPB, XPD, XPA and XPF) were localized in the normal cells and in the XP72TMA cells. **B.** Normal and XP101TMA cells. Row 1 – In the absence of UV, XPC and XPG protein was present in the normal cells (left and right images, red arrows). In contrast, in XP101TMA cells XPG protein was detected as diffuse staining (right image, yellow arrow,) but XPC protein was not detected. Row 2 – Following 100 J/m^2 UV irradiation through a 5μm filter, recruitment of XPC and XPG proteins was seen in the normal cells (red arrows). In the XP101TMA cells no XPC protein was detected and the XPG protein remained diffuse (right image,yellow arrow). C. Western blot of protein extracted from cells from normal (lane 1), XP101TMA (lane 2), XPH102TMA (lane 3) and XP72TMA (lane 4) using XPC (upper row) and beta-actin (lower row) antibodies. The ratio of the intensity of the XPC band to the actin band is shown.

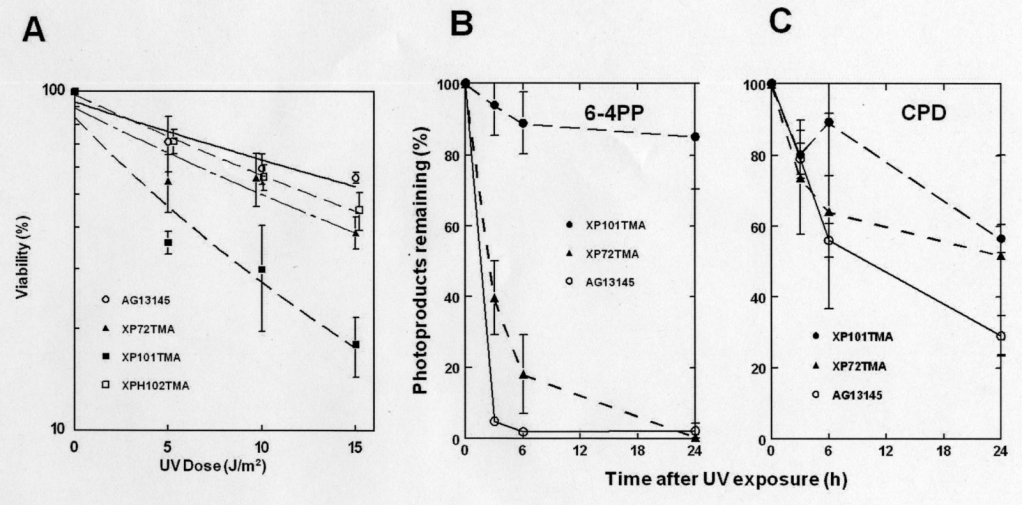

Figure 4.

Post-UV cell survival and removal of photoproducts. **A.** Post-UV viability of normal (open circles), XP101TMA (closed squares), XPH102TMA (open squares), and XP72TMA (closed triangles) fibroblasts measured by MTS assay. Mean + S.D. of quadruplicate cultures. **B.** Removal of 6-4 photoproducts from normal (open circles), XP101TMA (closed circles) and XP72TMA (closed triangles) cells following 10 J/m2 UV exposure measured by ELISA assay. **C.** Removal of CPD from normal (open circles), XP101TMA (closed circles) and XP72TMA (closed triangles) fibroblasts following 10 J/m^2 UV exposure measured by ELISA assay. The data presented as mean + S.D. of duplicate experiments for Normal and XP101TMA cells, but for XP72TMA cells the data are mean + S.D. of seven experiments (6-4PP) and six experiments (CPD).

Table 1

Real time quantitative RT-PCR detection of exon 4 inclusion and exon 4 skipping XPC mRNA in minigenes or cells

Minigene transfected into cells	Cells	XPC exon 4 inclusion (average fg[1])		XPC exon 4 skipping (average fg[1])		XPC exon 4 inclusion / skipping
pcDNA3.1-XPC-Normal BPS	XP4PA-SV	27550	100%[2]	5,985	22%	4.6
pcDNA3.1 -XPC-BPS mutant -24 position	XP4PA-SV	5185	19%	6,180	22%	0.8
pcDNA3.1 -XPC-BPS mutant -9 position	XP4PA-SV	1380	5%	3,485	13%	0.4
pcDNA3.1-empty vector	XP4PA-SV	1	0%	0.01	0%	-
Lipofectamine-treated only	XP4PA-SV	0.5	0%	0.001	0%	-
No treatment	XP4PA-SV	0.9	0%	0.028	0%	-
None	Normal[3,4]	171	100%[5]	4.3	3%	39.8
None	XP72TMA	5.5	3%	24.7	14%	0.2
None	XP101TMA	<0.1	<0.1%	47.9	28%	0.0

[1] All mRNA levels are expressed as fg of the standard plasmids. Only expressed mRNAs were measured by use of a forward primer in the vector sequence and a reverse primer in the XPC gene

[2] Per cent of mRNA expressed using normal minigene in the XP-C cells.

[3] KR06057 cells

[4] Levels of alternatively spliced endogenous XPC mRNA isoforms in cells from mildly- and severely-affected XP-C patients are from [Khan et al., 2004]

[5] Per cent of mRNA expressed in normal cells.